View metadata, citation and similar papers at core.ac.uk

brought to you by CORE

provided by Crossref

Strangeness at high μ_B

Recent data from FOPI and HADES

Yvonne Leifels[1,⋆]

[1] *GSI Helmholtzzentrum für Schwerionenforschung, Planckstr. 1, 64291 Darmstadt, Germany*

Abstract. Strangeness production in heavy-ion reactions at incident energies at or below the threshold in NN collisions gives access to the characteristics of bulk nuclear matter and the properties of strange particles inside the hot and dense nuclear medium, like potentials and interaction cross sections. At these energies strangeness is produced in multi-step processes potentially via excitation of intermediate heavy resonances. The amount of experimental data on strangeness production at these energies has increased substantially during the last years due to the FOPI and the HADES experiments at SIS18 at GSI. Experimental data on K^+ and K^0 production support the assumption that particles with an $\bar{s}$ quark feel a moderate repulsive potential in the nuclear medium. The situation is not that clear in the case of K^-. Here, spectra and flow of K^- mesons is influenced by the contribution of ϕ mesons which are decaying into K^+K^- pairs with a branching ratio of 48.9 %. Depending on incident energy upto 30 % of all K^- mesons measured in heavy-ion collisions are originating from ϕ-decays. Strangeness production yields - except the yield of Ξ^- - are described by thermal hadronisation models. Experimental data not only measured for heavy-ion collisions but also in proton induced reactions are described with sets of temperature T and baryon chemical potential μ_B which are close to a universal freeze-out curve which is fitting also experimental data obtained at lower baryon chemical potential. Despite the good description of most particle production yields, the question how this is achieved is still not settled and should be the focus of further investigations.

1 Introduction

The phase diagram of QCD usually presented in terms of temperature T and baryon chemical potential μ_B is in the focus of many experimental and theoretical investigations. At small baryonic chemical potentials the hadronic phase is assumed to be separated from the quark-gluon phase by a cross over transition. At a critical point the cross over transition is expected to evolve with rising baryonic chemical potential into a first order phase transition. At even higher baryonic chemical potential exotic states may appear.

Highest chemical potentials μ_B and moderate temperatures T at freeze-out can be accessed experimentally with heavy-ion collisions in the beam energy regime $E_{beam} < 6$ GeV/u (fixed target). In the course of these reactions, densities up to several times normal nuclear matter density ρ_0 are reached for relatively long times. The compressed nucleons are excited to heavier resonances, but the matter is still baryon dominated. Meson production is present but not prevailing. Most of the strange particles

⋆e-mail: Y.Leifels@gsi.de

© The Authors, published by EDP Sciences. This is an open access article distributed under the terms of the Creative Commons Attribution License 4.0 (http://creativecommons.org/licenses/by/4.0/).

are produced at or below their production thresholds in NN collisions. Production of strangeness at sub-threshold energies occurs in multi-step processes. Resonances or intermediate mesons (mainly π's) are utilized as energy reservoirs. Consequently, the production rates are very sensitive to densities reached in the course of those collisions and to in-medium effects, in particular the modification of life times and masses in the hot and dense nuclear matter.

Strangeness production at threshold has been studied at the BEVALAC in Berkeley and the SIS18 accelerator at GSI. Despite the low production yields of strange particles at or below threshold energies, modern detector set-ups capable to sustain high data rates are able to accumulate enough statics even on very rare probes.

After the pioneering experiments in Berkeley with the Streamer Chamber, the first set-up with which it was possible to gather high statistics on strange particles production below threshold was the KaoS spectrometer at SIS18. Equipped with a highly selective trigger and particle identification by magnetic rigidity it was possible to measure spectra of positive and negative Kaons within a small angular acceptance. The KaoS collaboration measured various systems in the energy regime available at SIS18. In particular, the Au+Au and C+C systems between 0.6 GeV/u and the highest energies available at GSI for these nuclei (1.5 Gev/u for Au and 2.0 GeV/u for C) have been investigated [1]. Due to the limited acceptance and the characteristics of the KaoS spectrometer, neutral mesons with open or hidden strangeness (like the K^0 or ϕ) or hyperons were not accessible. This was possible with the FOPI detector system at GSI having full azimuthal acceptance for particles emitted in the region of target to mid-rapidity. Measurement of directed flow of strange particles in a large acceptance and reconstruction on strange resonances decaying into charged products became available [2]. The HADES set-up is capable to record events with the highest rates achieved so far for heavy ion collision experiments in this energy regime. With the upgraded HADES detector high statistics data in a large acceptance is available, which allows to access observables which have been beyond the detection limit [3] of the former experiments.

Transport models are an essential tool to assess the physics of strange particles in the dense medium, and more precise measurements of strange particles help to confine the input parameters of the models. One particular result of the KaoS measurements is rather tight constraints on the nuclear matter equation of state at densities between 2-3 ρ_0. Theoretical models predict a strong dependence of the positive Kaon production on the nuclear equation of state. Since Kaons are mostly produced in multi-step processes at sub-threshold energies, the production is very sensitive to the number of collisions and – consequently – the density reached during the reaction. Theoretical models employing a soft or a hard nuclear equation of state predict quite different production yields for Kaons as function of beam energy. Experimental data from the KaoS collaboration and comparison to various model predictions yield a nuclear matter equation of state [4–6] which is rather soft.

In this contribution, the most relevant results on strange particle production of the GSI experiments are reviewed with special emphasis on the latest FOPI and HADES results

2 In-medium potentials

Modifications of hadron properties in dense baryonic matter are a current subject of intensive research in hadron physics. Various theoretical approaches [5, 8–10] agree qualitatively in predicting modifications of masses and coupling constants for kaons and anti-kaons. Kaons (K^+ and K^0) are expected to be subject to a repulsive potential, whereas antikaons (K^- and $\overline{K}^0$) should be attracted, see Fig. 1, where theoretical predictions for the density dependence of the kaon masses are presented [7]. The $\overline{K}^0$ is mixing with the K^0 to K^0_S and K^0_L. At the energies discussed here, the $\overline{K}^0$ contributes only little the K^0_S yield, and the measured K^0_S are considered to result from K^0 only. Mass and production threshold

energy for kaons should increase as a result of the in-medium KN interaction, whereas for antikaons the corresponding values should decrease substantially [7]. The in-medium modifications of kaonic properties have been already studied experimentally in terms of KN potentials and reported by several experiments focused on strangeness production at near-threshold energies [11–15].

2.1 Kaons

The first moment v_1 of the Fourier expansion to the azimuthal distributions $dN/d\Phi \propto 1 + 2v_1 cos(\Phi - \Phi_R) + 2v_2 cos(\Phi - \Phi_R) + ...$, where the azimuthal angle Φ is measured with respect to the reaction plane Φ_R is quantifying the directed side flow in a heavy ion reactions. In Fig. 2 values for v_1 measured by the FOPI collaboration in central Ni+Ni collisions at 1.9 AGeV are plotted as function of rapidity for positive and negative kaons and protons together with predictions of HSD [17] and IQMD [11] models. Near target rapidity K^+ - mesons show a collective in-plane deflection in the direction opposed to that of protons. This finding is in agreement with other data [18]. Models are able to describe this result when incorporating a slightly repulsive kaon nucleon (KN) potential of $U_{pot,KN}(\rho_0, \mathbf{k} = 0) \approx 20$ MeV, which is linearly depending on density (see Fig. 1). Calculations without an in-medium KN potential predict a smaller, close to isotropic directed flow. It should be noted that both models describe the proton flow in heavy-ion collisions in this energy regime and give consistent results for the strangeness production yields, despite the fact that the programs are conceptually different: IQMD is based on quantum molecular dynamics and HSD on a Boltzmann-Uehling-Uhlenbeck approach.

A similar result is obtained when comparing model predictions with K^0 spectra. In contrast to K^+ where the Coulomb interaction contribute to the repulsive potential, K^0 spectra are unbiased by this effect. In addition, they are detected by their decay into charged pions and can be measured down to very small momenta. In Fig. 3 HADES data for K^0 is presented. The momentum spectra of K^0 emitted close to mid-rapidity are shown and confronted with predictions of the IQMD model [11]. Again, the spectra are best described with a repulsive potential. The potential is estimated to be $U_{pot,KN} \approx +40$ MeV. Hence, HADES and FOPI results are showing the same trend, but are preferring slightly different potential heights. This discrepancy may be due to the different observables chosen or due to other input parameters of the models, e.g. production or re-scattering cross sections of Kaons. Those need to be confined by further systematic measurements.

The HADES collaboration recently measured Au+Au collisions at 1.25 AGeV with very high statistics, which allowed to reconstruct phase space distributions of charged and uncharged Kaons. The low momentum part of K^0 spectra is well described by IQMD model predictions employing the same input parameters as for the light system and the same kaon nucleon potential [19]

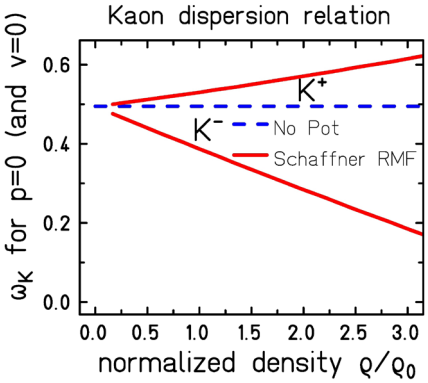

Figure 1. In-medium kaon energy $\omega(\mathbf{k} = 0)$ as function of baryon density fitted to reproduce the calculations of [7]: $\omega(\mathbf{k}, \rho) = \sqrt{(\mathbf{k} - \mathbf{\Sigma_v})^2 + m^2 + m\Sigma_s} \pm \Sigma_v^0$ with a scalar self energy Σ_s and a vector self energy $(\Sigma_v^0, \mathbf{\Sigma_v})$, where the sign of the vector term $\pm\Sigma_v^0$ is positive for kaons and negative for antikaons.

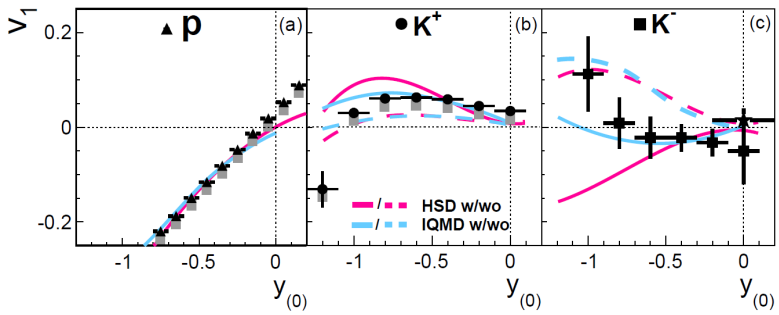

Figure 2. FOPI Results for directed flow v_1 of kaons in comparison to the flow of protons as a function of the center-of-mass rapidity $y_{c.m.}$. Solid lines are predictions using the HSD transport code.The v_1 - values are obtained within the acceptance of the CDC, for details see text. Data taken from [16]

2.2 Antikaons

In contrast to the situation for kaons where the question of the in-medium potential seems to be essentially settled, the antikaon nucleon potential is not so easy to assess. Due to the existence of a resonance, the $\Lambda(1405)$, close to the K^-p threshold a non-perturbative treatment is required in theoretical models. Theoretical predictions for the $\bar{K}N$ potential differ substantially, therefore. Kaonic atoms confirm that the $\bar{K}N$ interaction is attractive at small momenta and low densities but its strength at larger densities is less constrained. On the other hand, antikaons are predicted to be produced via the strangeness exchange reaction $\Lambda + \pi \rightarrow K^- + N$. Hence, their production is closely following that of the K^+. Additionally, K^- are strongly absorbed in the nuclear medium, a process which partially covers the effect of the potential. Microscopic transport models employing an attractive density dependent with $\bar{K}N$ potential $U_{pot,\bar{K}N}(\rho_0, \mathbf{k} = 0) = 50 - 90$ MeV predict: a) the spectra show a steeper slope as compared to kaons, i.e. a smaller apparent temperature, b) the flow signals v_1 and v_2 are modest. Those predictions indeed describe the experimental data reasonably well, antikaon multiplicities as well as antikaon spectra. In the right panel of Fig. 2, directed flow v_1 of K^- measured by the FOPI collaboration is compared to model predictions with and without employing an attractive, density dependence $\bar{K}N$ potential $U_{pot,\bar{K}N}(\rho_0) = 50$. In HSD, a G-Matrix approach is used for obtaining the $\bar{K}N$ potential and particles are propagated off-shell, whereas in IQMD the antikaons are treated as quasi-particles subject to a potential taken from [21] and during the production process the free production cross section is taken at $\sqrt{s}$ modified by the in-medium mass of the K^-. Both models

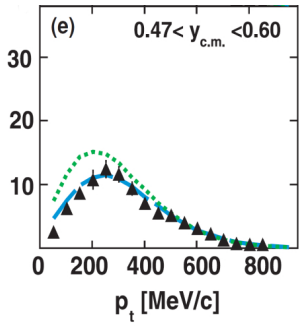

Figure 3. HADES results on K^0 production at mid-rapidity in Ar+KCl collisions at 1.76 GeV/u in comparison to IQMD model calculations. The blue line represents model predictions employing a KN potential with the height of $U_{pot,KN} = +40$ MeV and the green dotted line predictions without an explicit KN potential.

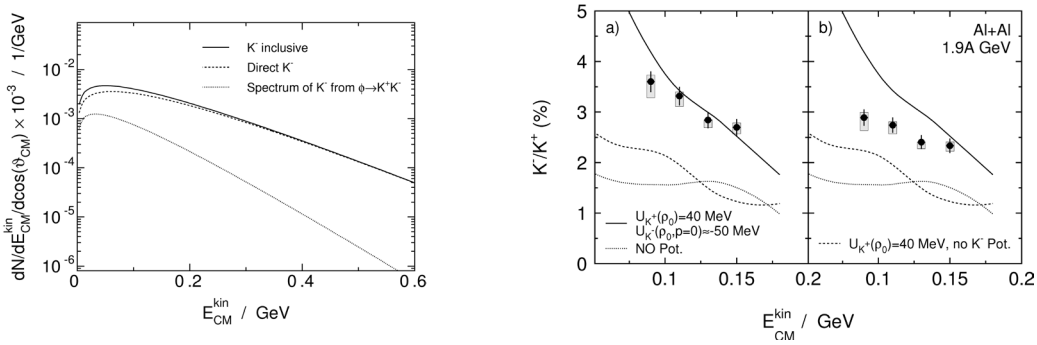

Figure 4. Left panel: Kinetic energy distributions of K^- mesons obtained by the inclusive fit to the experimental data (solid line), K^- from ϕ meson decays (dotted line), and "direct" K^- mesons generated from the thermal source (dashed line). See text for details. Right panel: a) the K^-/K^+ ratio as a function of $E_{k,CM}$ in the Al+Al experiment. Error bars represent statistical uncertainties. Grayed rectangles represent the estimation of systematical errors. Lines represent results of HSD model predictions including different values of KN potentials. b) the K^-/K^+ ratio distribution corrected for K^- mesons from ϕ decays. Grayed rectangles do not include the uncertainties of T_{eff,K_ϕ}. Data from [20].

differ in predicting v_1 in the target rapidity region, but the large statistical error of the experimental data prevents to distinguish between the two.

However, precise in-medium modification studies have to account for feeding of the K^- emission yield by the $\phi(1020)$ meson decays. A comparison of the mean free path of the latter particles, $c\tau_\phi \approx 50$ fm, to the average duration of the hot and dense collision zone (20-30 fm/c) suggests that most ϕ mesons decay outside this zone. It should be also noted, that the ϕ meson mass is only 32 MeV/c^2 larger than that of a K^+K^- pair. Thus, a substantial coupling of the ϕ and K^- dynamics is expected. In addition, K^- originating from the ϕ meson decays are governed by different kinematics than those emitted directly from the collision zone.

For light to intermediate heavy systems colliding at beam energies of 1.7–1.9 GeV/u it is found that about 20% of the K^- mesons originate from ϕ meson decays [22–24]. The contribution of the ϕ is seemingly larger at lower beam energies. It measured to be 30% for 1.25 AGeV Au+Au collisions [19]. Hence, the contribution of ϕ mesons has to be considered in the models. Neither HSD nor IQMD are reproducing the high ϕ yields measured experimentally. Instead, a simple two source model for antikaon production is used to disentangle the two contributors to the K^- phase space distributions.

- the inclusive K^- emission spectrum is isotropic (an assumption which is justified by experimental data) and described by a Boltzmann distribution with the parameter T_{eff,K^-}
- K^- mesons from ϕ meson decays and observed in the experiment are produced outside the collision zone.
- both the "direct" and the ϕ meson sources of K^- are characterized by Boltzmann distributions, with parameters: $T_{\mathrm{eff},K_{\mathrm{direct}}}$ (unknown, to be found), T_{eff,K_ϕ} (from experimental data), and the normalization factors weighting the inclusive K^- emission probability according to the found ϕ/K^- ratio.

The results of this procedure are presented in the left panel of Fig. 4 which shows the total kinetic energy distribution of K^- mesons in Al+Al collisions at 1.9 AGeV, and its two respective components. The "direct" component was obtained by subtracting the contribution from the ϕ meson decays from the inclusive spectrum.

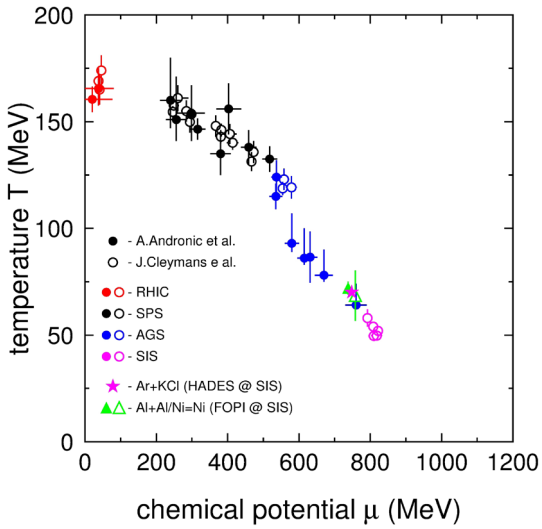

Figure 5. Statistical hadronisation model results for various incident energies and systems. Data are taken from various references. The low energy (SIS18) data are from [20, 24, 27].

The experimentally observed difference between K^+ and K^- inverse slope parameters can be partially explained by this effect. HADES claims that the ϕ decay accounts for the whole T_{eff} difference in Ar+KCl collisions at 1.7 AGeV [22] and Au+Au at 1.2 AGeV [19], in Al+Al and Ni+Ni collisions at higher energies it only accounts for approximately half the temperature difference [20, 24]. As consequence, the determination of the $\bar{K}N$ requires models which also reproduce the ϕ production yields. With the UrQMD model [25] it is possible to reproduce measured ϕ yields, but it is lacking potentials.

3 Chemical and kinetic freeze-out

Statistical hadronisation models are able to describe production yields of strange particles with essentially three parameters: temperature T, baryon chemical potential μ_B and a parameter describing the volume of the source R_V. In the limit of high temperature and/or large systems, the grand-canonical treatment of strangeness is adequate, but at low energies strangeness has to be implemented exactly in the canonical ensemble. This is achieved by introducing a strangeness correlation radius, $R_C < R_V$,

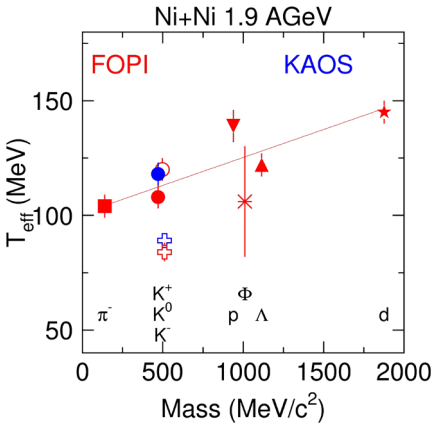

Figure 6. Effective temperatures T_{eff} measured for various particles emitted at mid-rapidity in Ni+Ni collisions at 1.9 AGeV as function of the particle mass. Data from KaoS (blue symbols) and FOPI (red symbols) are shown.

which is determined from experimental data. With the exception of the double strange Ξ^- hyperon [26, 27], the production yields can be reproduced within statistical models with parameters which fall reasonably well on the universal freeze-out curve (see Fig. 5). However, some of the investigated systems (e.g. Al+Al by FOPI) are rather small and the assumption of complete equilibration questionable.

Kinetic freeze-out shows a more complicated pattern which can be seen in Fig. 6, where inverse slope parameters T_{eff} of spectra at mid-rapidity are shown for various particle species emitted in central Ni+Ni collisions at 1.9 GeV/u. Data from the FOPI and KAOS collaborations are compiled [24, 28], for π's only the inverse slope parameter of the high momentum part of the spectra are shown because the low momentum part is influenced by the decay of Δ resonances. The inverse slope parameters for π, protons and deuterons is rising with mass, which is interpreted as signal of a collective radial flow. In lighter systems this effect vanishes because of the diminished pressure built-up, whereas it is more pronounced in heavier systems.

It is not obvious that the strange particles do follow this trend apart from the K^+: kaons with anti-strangeness $K^{+,0}$ and kaons with strangeness K^- have significantly different temperatures. Three explanation have been offered to account for the lower K^- temperatures: the influence of the $\bar{K}N$ potential, the contribution of the ϕ decay, and - inspired by a thermal picture - different freeze-out times. The latter is motivated by the fact that most of the K^- production at sub-threshold energies will proceed via strangeness exchange in hyperon-pion reactions. Hence, K^- will appear after the production of K^+ when the collision system already have cooled down. Within a microscopic picture, both the decay of the ϕ and the attractive $\bar{K}N$ potential will yield lower T_{eff} for the K^- than for the K^+ (see discussion in Section 2.2)

The experimental T_{eff} of the ϕ is of the same magnitude as that of the K^+ but not as high as the inverse slope parameter of the protons. Regarding the large experimental error bars it is necessary to measure the ϕ mesons with higher statistics in the future, as well as to study the interaction processes of the ϕ with nucleons, i.e. re-scattering and absorption cross sections.

The inverse slope parameter of the Λ is smaller than that of the protons. This in accordance with the predictions of microscopic models: the Λ is produced when the compressed collision zone has already expanded and the temperature has slightly decreased, and the subsequent elastic collisions of the Λ with the surrounding nucleons are insufficient to rise the inverse slope parameter T_{eff} to the level of that of the nucleons. The spectral distributions of Λ measured at different energies and system sizes may give access not only to the in-medium ΛN cross sections but also to ΛN potential in dense matter.

4 Conclusion

New experimental data and observables in comparison to state-of-the-art microscopic models give access to the KN in-medium potential. On the other hand the $\bar{K}N$ potential is not easily accessible in heavy-ion reactions, new experimental observables and approaches have to be found. One possibility is to investigate correlated K^+K^- production in elementary and heavy-ion reactions and exclude the ϕ from the analysis. Such a procedure has been suggested by the ANKE collaboration [29]. Additional high statistics data of strangeness production as a function of energy and system size is necessary for continuing such type of analyses and constraining further the input parameters in the microscopic models. Supplementary elementary p+A and π+A data are important to investigate the role of heavy resonances.

There are two model approaches to strangeness production at sub-threshold energies leading to puzzling results: in-medium modifications of the kaon masses are required to describe the experimental data in microscopic models, whereas statistical hadronisation models reproduce production

yields with vacuum masses. Generally, all measured particle yields in heavy-ion reactions at SIS energies can be described within thermal models with the exception of the Ξ^- data. On the other hand, it has been shown that the particle ratios measured in heavy-ion collisions can also be reproduced by microscopic models like UrQMD [25]. If microscopic transport models also reproduce the difference between kinetic and chemical temperatures (including the gross properties of the reactions like stopping and flow), one might investigate the mechanisms leading to the apparent thermal equilibration in heavy-ion reactions within those models. A key issue for this might be the analysis of interdependencies in the production of different particle species. For instance, it has been suggested that strangeness exchange may cause the experimentally observed proportionality between the beam energy dependence of the K^-/K^+ and π/A ratios below 10 GeV/u; here A is the system size [11].

The investigation of strange particles produced close to their threshold in NN collisions will be continued at SIS18 with HADES and later at FAIR with the Compressed Baryonic Matter CBM.

References

[1] P. Senger et al., Nucl. Instr. Meth. Phys. Res. A **327**, 393 (1993).
[2] J. Ritman *et al.*, Nucl. Phys. B (Proc. Suppl.) **44**, 708 (1995)
[3] G. Agakishiev *et al.*, Eur. Phys. J. A **41**, 243 (2008).
[4] J. Aichelin and C.M. Ko, Phys. Rev. Lett. **55**, 2661 (1985)
[5] C. Fuchs, Prog. Part. Nucl. Phys. **56**, 1 (2006).
[6] C. Hartnack, H. Oeschler, and J. Aichelin, Phys. Rev. Lett. **90**, 102302 (2003)
[7] J. Schaffner-Bielich, J. Bondorf, I. Mishustin,
[8] G.E. Brown, and M. Rho, Phys. Rev. Lett. **66**, 2720 (1991)
[9] W. Weise, Nucl. Phys. A **610**, 35c (1996)
[10] M.F.M. Lutz, Prog. Part. Nucl. Phys. **53**, 125 (2004).
[11] C. Hartnack, H. Oeschler, Y. Leifels, E. Bratkovskaya, J. Aichelin, Phys. Rep. **510**, 119 (2012).
[12] Y. Shin *et al.* [KaoS Collaboration], Phys. Rev. Lett. **81**, 1576 (1998)
[13] K. Wiśniewski *et al.*, Eur. Phys. J. A **9**, 515 (2000).
[14] F. Uhlig *et al.* [KaoS Collaboration], Phys. Rev. Lett. **95**, 012301 (2005)
[15] M.L. Benabderrahmane *et al.* [FOPI Collaboration], Phys. Rev. Lett. **102**, 182501 (2009).
[16] V. Zinyuk *et al.*, Phys. Rev. C **90**, 025210 (2014).
[17] W. Cassing, L. Tolos, E. L. Bratkovskaya and A. Ramos, Nucl. Phys. A **727**, 59 (2003)
[18] P. Crochet *et al.* [FOPI Collaboration], Phys. Lett. B **486**, 6 (2000)
[19] H. Schuldes *et al.*, Contribution to this conference
[20] P. Gasik *et al.*, Eur. Phys. J. A **52**, 177 (2016)
[21] C. M. Ko and G. Q. Li, J. Phys. G **22** (1996) 1673
[22] G. Agakishiev *et al.*, Phys. Rev. C **80**, 025209 (2009).
[23] M. Lorenz, PoS (BORMIO 2010), 038.
[24] K. Piasecki *et al.*, Phys. Rev. C **91**, 054904 (2015).
[25] J. Steinheimer and M. Bleicher, J. Phys. G **43** 015104 (2015)
[26] M. Merschmeyer *et al.* [FOPI Collaboration], Phys. Rev. C **76** 024906 (2007)
[27] G. Agakishiev et al., Eur. Phys. J. A **52**, 178 (2016).
[28] A. Förster *et al.*, Phys. Rev. Lett **91** 152301 (2003)
[29] E. Paryev *et al.*, J. Phys. G **42**, 075107 (2015)